Progress in Physics of Applied Materials 3 (2023) 49–55

Semnan University

Progress in Physics of Applied Materials

journal homepage: https://ppam.semnan.ac.ir/

A Study on Structural, Optical, and Magnetic Properties of $ZnO/ZnFe_2O_4$ Composite

M. Saidi, M. E. Ghazi*, M. Izadifard

Physics department, Shahrood University of Technology, Shahrood, Iran

ARTICLE INFO

Article history:
Received: 19 June 2023
Revised: 22 July 2023
Accepted: 5 August 2023

Keywords:
Hydrothermal method
$ZnO/ZnFe_2O_4$ nanocomposite
magnetic properties
optical properties

ABSTRACT

In this research, $ZnO/ ZnFe_2O_4$ nanocomposites with a weight ratio (1:1) were made using hydrothermal method and annealing temperatures of 600°C and 700°C. Structural, optical, and magnetic properties of the synthesized powders were characterized using X-ray diffraction (XRD), field emission scanning electron microscope (FESEM), ultraviolet-visible spectrometer, and vibrating sample magnetometer (VSM). The results obtained from the XRD diffraction patterns confirmed the formation of the mixed phases, hexagonal zinc oxide and cubic spinel phases of pure zinc ferrite. FESEM images showed that with the increase of annealing temperature, the samples have a cohesive and agglomerated structure. The measurement of the absorption spectra of the synthesized samples showed that the absorption in the visible region increases with increase in annealing temperature. The optical band gap value for the $ZnO/ZnFe_2O_4$ composites were in the range of 2.1-2.2 eV which is between the band gap values of ZnO (3.37 eV) and zinc ferrite (1.8 eV). The hysteresis loops measured with VSM indicated a soft and weak ferromagnetic magnetic behavior for both samples.

1. Introduction

Hybrid nanostructures composite are recently attracting considerable attention in multifunctional nanomaterial design[1]. This popularity is due to the ability of these hybrid nanostructures to not only retain the basic characteristics properties of the individual components but also some unique multi-functionality. More importantly, the interaction between the two components of the composite endowing them with much improved properties[2]. These improvements include enhanced spin interactions, decrease the band gap and increasing the optical absorption range, chemical stability and prolonged lifetime[3].

Hybrid nanostructures offer great opportunities for applications in areas such as biomedicine, renewable energy, catalysis, information processing, and data storage devices[4]. Recently, ZnO-based nanostructures have received attention due to their excellent performance in various applications.

Zinc oxide is considered as one of the most important II-VI group semiconductor due to having a direct and wide band gap (about 3.37 eV at room temperature), high exciton energy (60 meV), central asymmetric structure, and ease of synthesis is recognized in scientific research and technological applications [5]. However, it has fast electron-hole recombination and has poor performance in the visible light wavelengths due to its wide band gap value [6, 7]. One promising approach for realizing the practical application of ZnO and improving its properties is the combination of ZnO with other semiconductors to form hybrid nanostructures[8]. Especially, compositing it with magnetic nanomaterials alters its electronic and magnetic properties because of interaction among delocalized 'sp' electrons of ZnO and 'd' electrons of magnetic nanomaterials[9].

Among the magnetic nanomaterials, spinel ferrite nanomaterials are characterized by their high electrical resistivity, high saturation magnetization, low eddy current, and low cost which is widely used in memories storage, a drug targeted delivery, magnetic resonance imaging, photo-catalysis, and other fields. The general formula of spinel ferrite material is MFe_2O_4, where M can be Co^{+2}, Ni^{+2}, Mn^{+2}, Zn^{+2}, and other divalent metal ions that are in the tetrahedral sites, while trivalent Fe ions are in the

* Corresponding author. Tel.: 00982332395270
E-mail address: mghazi@shahroodut.ac.ir

DOI: 10.22075/PPAM.2023.30980.1057

octahedral site. $ZnFe_2O_4$ is an n-type semiconductor, which can be used as an alternative material suitable for optical purpose because of its relatively small band gap (about 1.8-2.2 eV), non-toxic, and stable chemical properties[10]. $ZnFe_2O_4$ and ZnO can form n–n homo-type heterojunction, which hinders the recombination of photo-generated electron–hole pairs and improves the utilization ratio of carriers [6]. In recent years, $ZnO/ZnFe_2O_4$ nanocomposites have been synthesized using different methods such as co-precipitation [11], hydrothermal [4], and sol-gel [12] for various applications.

The main purpose of this research was to use the heterogeneous bonding of zinc oxide with zinc ferrite in order to combine semiconducting and magnetic properties and improving the physical properties of the composite compared to the pure zinc oxide and zinc ferrite nanostructures. In this work $ZnO/ZnFe_2O_4$ composites were prepared by a hydrothermal precipitation method. Then their structural, morphology, optical, and magnetic properties were investigated using appropriate characterization methods.

2. Experimental

To prepare the ZnO powder, first a specific amount of zinc acetate dihydrate ($Zn(CH_3CO)_2,2H_2O$) dispersed in deionized water ultrasonically for 20 minutes to prepare a 0.3 M zinc acetate dihydrate solution. Then urea was added to the above solution to adjust the pH (about 7) and it was stirred by a magnetic stirrer at a speed of 400 rpm at ambient temperature. The resulting clear solution was poured into a Teflon coated autoclave. The autoclave was placed in a chamber oven at 120°C for 5 hours. The obtained powder was washed several times with distilled water and ethanol to remove salt and other impurities. The powder was dried at room temperature and annealed at 500°C for 3 hours in a tube oven.

In order to prepare a nanocomposite samples with the composition ratio (1:1), ZnO nanoparticles powder (1gr) without annealing and 1 gr of iron nitrate ($Fe(NO_3)_3,9H_2O$) mixed in 40 ml deionized water in an ultrasonic device for 20 min. The synthesis conditions were the same as previous section. Finally, the resulting precipitate was annealed for 3 hours at 600°C and 700°C under laboratory atmospheric conditions in a tube furnace and named ZF-600 and ZF-700 respectively.

3. Characterization methods

In order to investigate the structural characteristics of the powder samples synthesized by hydrothermal method, their X-ray diffraction data were recorded by a $Cu_{k\alpha}$ beam with wavelength of 1.5404 Å at an angle range of 2θ=10°-80° with a step size of 0.05°. In order to check the morphology of the sample, a field effect scanning electron microscope (ZEISS) was used to record images from the surface of the powder samples. The optical properties of the samples were studied using a Shimadzo model 1800 visible-ultraviolet spectrometer. The magnetic properties of the samples were also measured with a vibrating sample magnetometer (VSM).

4. Results and discussion

X-ray diffraction patterns for ZF-600 and ZF-700 nanocomposite samples prepared at annealing temperatures of 600 °C and 700 °C are shown in figure 1. The patterns show diffraction peaks from planes (100), (002), (101), (102), (110), (103), (200), (112), and (201) of ZnO Wurtzite structure according to the standard card number 01-075-0576, and the lattice constant of a=b=3.2427Å and c=5.1948 Å. Also the patterns illustrate diffraction peaks at angles 18.2, 29.91, 35.31,42.81,53.31, 56.81, and 62.31º from the diffraction planes (111), (220), (311), (400), (422), (511), and (440) respectively, for cubic $ZnFe_2O_4$ spinel structure in accordance with the standard card number 00-001-1108 with a=b=c =8.43Å without any impurity phase.

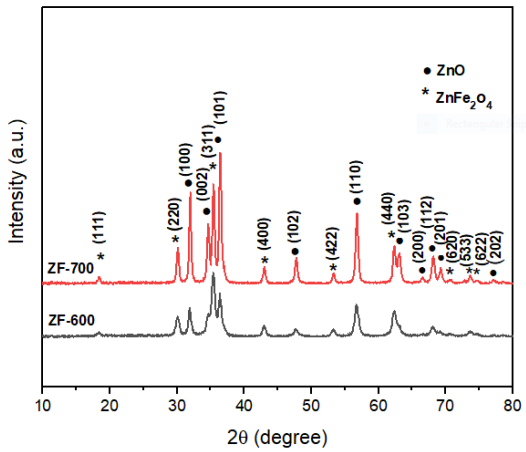

Fig. 1. XRD patterns for nanocomposite samples ZF-600 and ZF-700.

The average value of crystallite size (D_s) obtained from Scherrer equation for ZF-600 and ZF-700 nanocomposite samples (at annealing temperatures of 600 °C and 700 °C) is listed in Table1.

In addition, the XRD patterns show that by increasing the annealing temperature, the peak of full width at half maximum (FWHM) for ZF-700 sample is narrower compared to corresponding value for the ZF-600 sample showing increase in crystallite size.

In order to account the strain in the peak broadening of the samples, the Williamson-Hall equation was used:

$$\beta \cos\theta = \frac{0.9\lambda}{D} + 4\varepsilon \sin\theta \qquad (1)$$

In this relation λ is the wavelength of X-rays equal to 1.54056 Å, β is the full width of the diffraction peak at half maximum and θ is the Bragg diffraction angle [13]. By drawing β Cosθ versus 4Sinθ and a linear fitting of the data, the average crystallite size (D_w) and the microscopic strain (ε) was estimated. The Williamson-Hall diagrams are shown in figure 2.

To draw these diagrams, six diffraction peaks (100), (002), (101), (102), (110) and (103) for ZnO sample and four diffraction peaks (111), (220), (311), and (400) for the $ZnFe_2O_4$ sample were used. The values obtained for the average crystallite size and the microscopic lattice strain are reported in Table 1. The ferrite phase of the ZF-700

sample has the largest crystallite size and the lowest strain, therefore it has better crystallinity. As expected with increasing the annealing temperature, the average crystallite sizes of the zinc ferrite and ZnO phases increase and the amount of strain decreases.

The reduction in crystal lattice strain can be attributed to factors affecting crystallites such as crystal defects, dislocations, and grain boundaries. Normally increase in annealing temperature causes grain growth and reduction of the grain boundaries which affects the crystal properties. Also, when the annealing temperature increases, the crystal defects decrease and so the lattice strain. In general, the presence of more strain in a composite structure (larger lattice mismatch) leads to more instability.

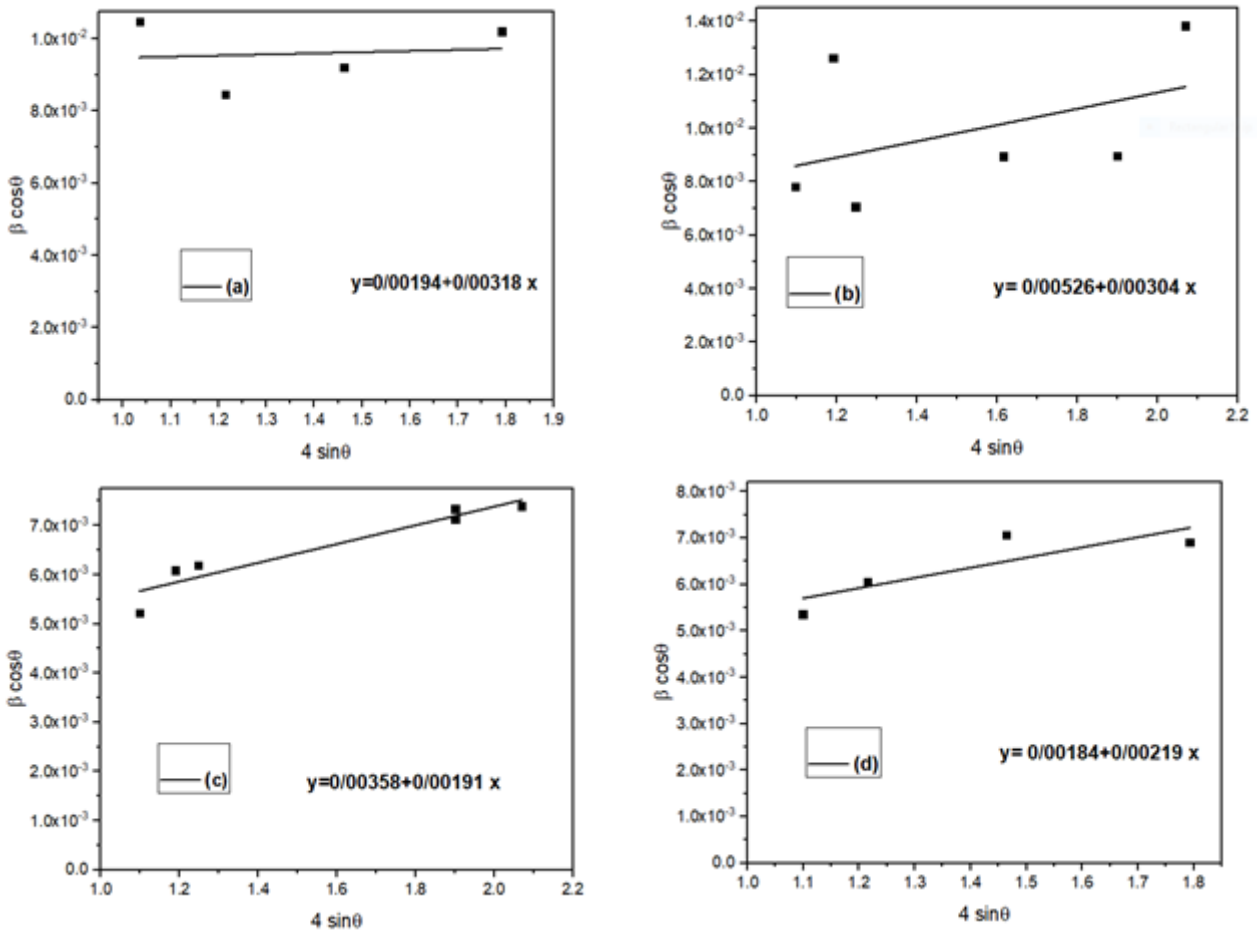

Fig. 2. Williamson-Hall diagrams for the ZF-600 sample: a: $ZnFe_2O_4$ phase and b: ZnO phase and ZF-700 sample: c: $ZnFe_2O_4$ phase and d: ZnO phase.

Table 1. Data extracted from the X-ray diffraction patterns of the ZF-600 and ZF-700 samples.

Sample	Phase	D_s (nm)	D_W (nm)	ε ($\times 10^{-3}$)	a (Å)	c (Å)
ZF-600	ZnO	18.3	26.3	0.760	3.231	5.218
	$ZnFe_2O_4$	32.5	71.4	0.795	8.241	----
ZF-700	ZnO	27.1	38.7	0.477	3.249	5.215
	$ZnFe_2O_4$	34.6	75.2	0.547	8.440	---

5. Surface morphology

FESEM images of nanocomposites annealed at different temperatures in two scales of 100 nm and 1 μm are shown in Figure 3. The images show the grains have almost a spherical shape that is stuck together and agglomerate. By increasing the annealing temperature from 600 °C to 700 °C, an accumulation of almost spherical nanocomposite with average grain diameter of 47.5 nm and 50.4 nm was observed for ZF-600 and ZF-700 samples respectively. It is obvious that increasing the annealing temperature increased the grain size.

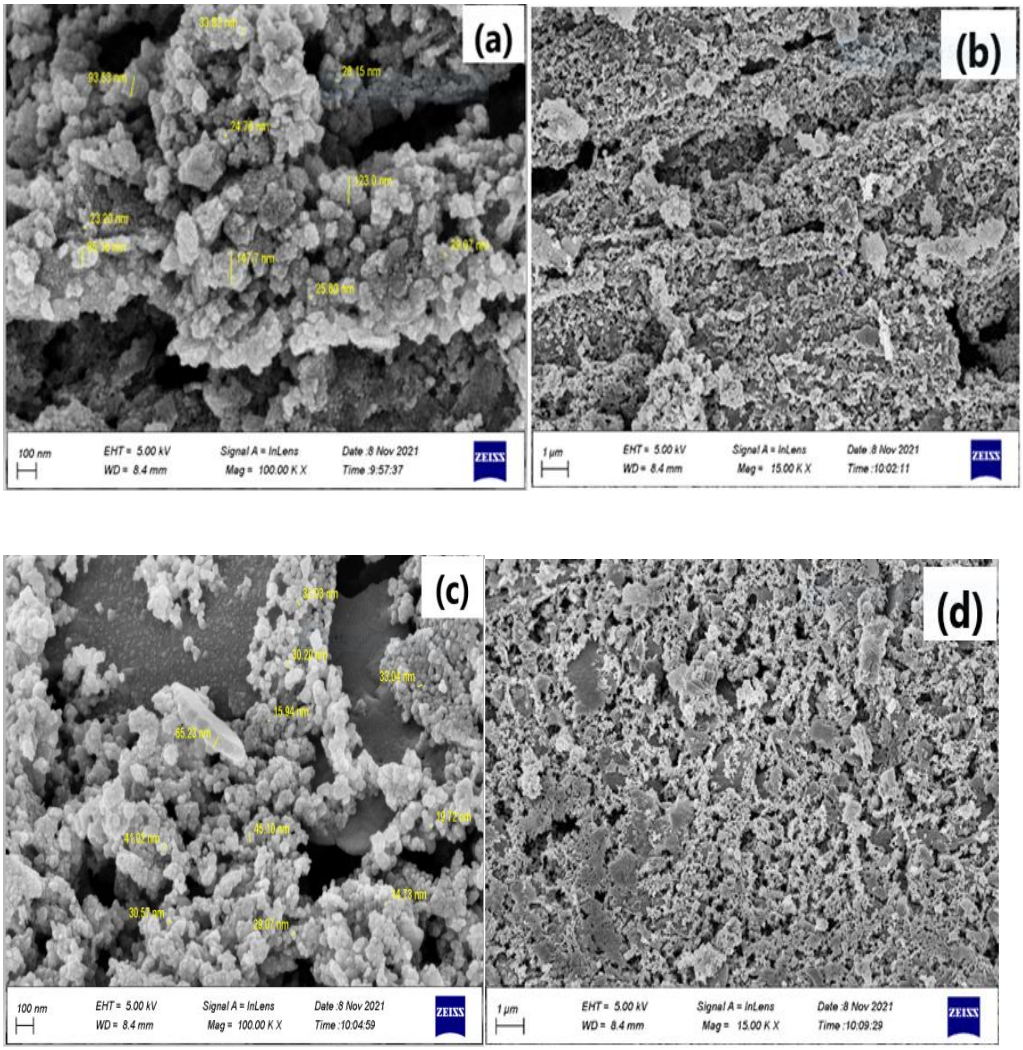

Fig. 3. FESEM images of samples (a) and (b)ZF-600, (c) and (d) ZF-700 in two scales of 100 nm and 1 μm.

6. Optical properties

Fig. 4 shows the absorption spectra of the nanocomposites (wavelengths of 300-1100 nm) at room temperature in the UV-vis region. It can be seen that both samples have the ability to absorb light in the visible region. The absorption is higher in the ZF-600 sample compare to the ZF-700 sample probably due to the smaller crystallite size of the constituent parts of the composite.

The light absorption edge of the $ZnO/ZnFe_2O_4$ at an annealing temperature of 600 °C is located at a wavelength of around 560 nm and this value for the ZF-700 sample is approximately 590 nm. In other words, with the increase in the annealing temperature, the absorption edge has moved to larger wavelengths (red shift) [14]. To determine the band gap values of the samples, the following Tauke equation was used [15]:

$$(Ahv)^m = K(hv - E_g) \quad (2)$$

Where A is the absorption, hν is the incident photon energy, K is a constant, E_g is the band gap energy, and m has the values of 2 and 0.5 for the direct and indirect gap respectively. As the ZnO is a direct wide band gap semiconductor and the $ZnFe_2O_4$ has both direct and indirect band gap values (but with only 0.1 eV difference), so we considered calculating the direct band gap. $(Ahν)^2$ as a function of the photon energy (hν) was plotted for both the samples and shown in figure 5.

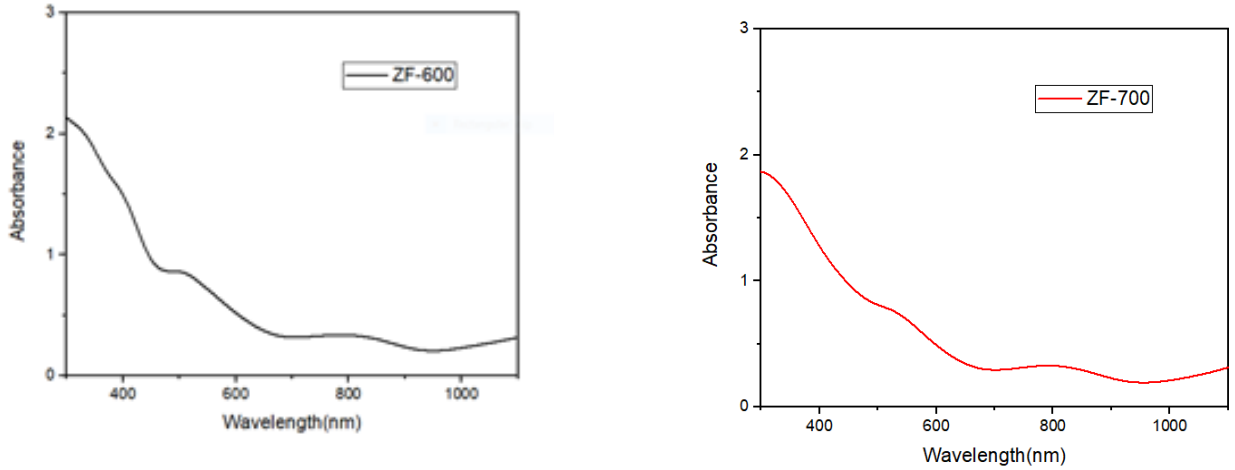

Fig. 4. Absorption spectra of the nanocomposite samples, ZF-600 and ZF-700.

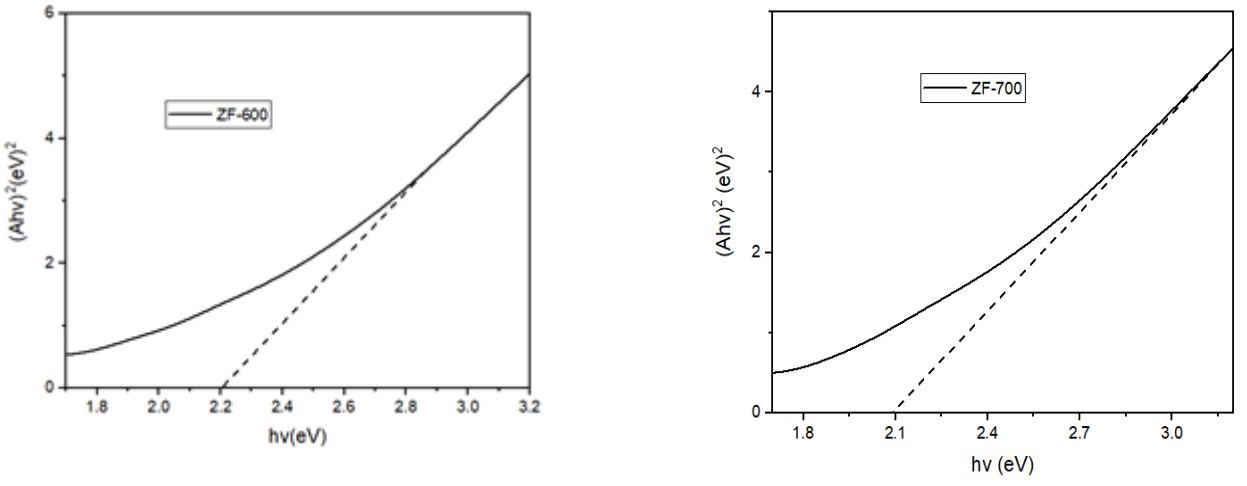

Fig. 5. *(Ahν)²* versus *hν* curves to calculate the direct band gap of the samples.

The amount of direct energy gap was obtained through the slope of the liner part of the curve and its intersection with the hν axis. Band gap values for ZF-600 and ZF-700 nanocomposite samples were found to be about 2.2 and 2.1 eV respectively. The band gap of nanocomposites decreased with increasing the annealing temperature that could be due to the bigger crystallite size of ZF-700 and growing the $ZnFe_2O_4$ phase in the composite with smaller band gap energy about 1.8 eV [10,16].

According the band gap values of the nanocomposites, these samples can be suitable for improving the photocatalytic activity in the visible light region.

7. Magnetic properties

Figure 6 shows the hysteresis loops of the ZF-600 and ZF-700 samples. The samples were examined in the applied magnetic field (room temperature) in the range of -10000 to 10000 gauss. The figure shows soft week ferromagnetic behavior for both samples at room temperature. Generally, Zinc oxide is diamagnetic because two electrons escape out from the 4s orbital in case of Zn^{2+} but the 3d orbital remains filled with paired electrons making it diamagnetic. In some studies, weak ferromagnetic properties due to the presence of vacancies have been reported. The values of magnetic parameters of the ZF-600 and ZF-700 samples are reported in Table 2. The result indicates that with increasing the annealing temperature from 600 °C to 700 °C, a small reduction of magnetic parameters occurred.

Singh Yadav et al. [17] have investigated the effect of annealing temperature on $ZnFe_2O_4$ nanoparticles. They observed an increase in crystallite size with increasing annealing temperature and measurements of magnetic properties showed that saturation magnetization decreases with increasing annealing temperature. They stated that the ferromagnetic property of this compound comes from migration of some iron ions to the tetrahedral sites, which causes a strong super-exchange interaction between the tetrahedral and octahedral site cations.

The data in Table 2 shows similar trend with reference 17 and a small reduction of magnetic parameters may also be originated from enhancement of crystallinity of the nonmagnetic ZnO phase at higher annealing temperature as the XRD data indicates. P. Falak et al. reported ZnO-$ZnFe_2O_4$ nanoparticles calcined at 600 and 800 °C show paramagnetic–superparamagnetic type behavior [7]. Theirs measured remanence magnetization values are about 0 emu/g for the samples calcined at 600 and 800 °C

but this value is about 0.8 emu/g for those calcined at 400 °C. As can be seen, the magnetization of the samples decreased by increasing calcination temperature.

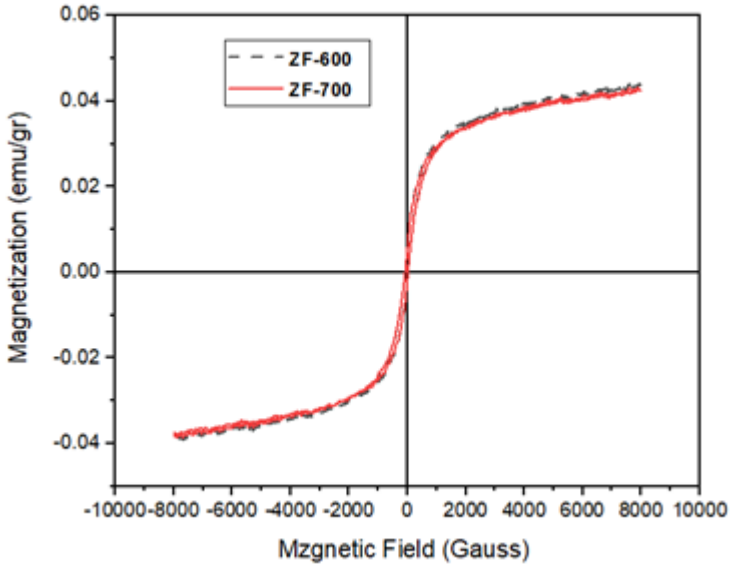

Fig. 6. Magnetic hysteresis curves for nanocomposite samples ZF-600 and ZF-700.

Table 2: Values of magnetic constants extracted from the magnetic hysteresis curves of ZF-600 and ZF-700 samples.

sample	M_{max} (emu/gr)	M_r(emu/gr)	H_C(G)
ZF-600	0.044	0.00613	42.5
ZF-700	0.042	0.00611	41.5

8. Conclusions

$ZnO/ZnFe_2O_4$ nanocomposites with the same weight ratio were synthesized by hydrothermal method. The samples were annealed at 600°C and 700°C to confirm the formation of the $ZnO/ZnFe_2O_4$ composite crystal structure. The recorded X-ray diffraction patterns of the samples confirmed the presence of peaks corresponding to the hexagonal phase of ZnO and the cubic structure of pure $ZnFe_2O_4$. FESEM images showed that increasing the annealing temperature increases the grain size. The study of optical property showed a red shift with increasing of the annealing temperature The extracted direct band gap values are around 2.1-2.2 eV, much lower than ZnO band gap value making this composite suitable for photovoltaic application. The magnetic measurements revealed a weak ferromagnetic behavior for both samples. The result indicates that with increasing the annealing temperature from 600 °C to 700 °C, a small reduction of magnetic parameters occurred.

References

[1] S.K. Noukelag, F. Cummings, C. J.Arendse, M. Maaza, "Physical and magnetic properties of biosynthesized ZnO/Fe2O3, $ZnO/ZnFe_2O_4$, and $ZnFe_2O_4$ nanoparticles." Results in Surfaces and Interfaces 10 (2023)100092.

[2] G. Tong, F. Du, W. Wu, R. Wu, F. Liu, Y. Liang, "Enhanced reactive oxygen species (ROS) yields and antibacterial activity of spongy $ZnO/ZnFe_2O_4$ hybrid micro-hexahedra selectively synthesized through a versatile glucose-engineered co-precipitation/annealing process." Journal of Materials Chemistry B 1(2013) 2647-2657.

[3] B.Z. Hsu, C.L. Yu, S. Sakthinathan, T.W. Chiu, B.S. Yu, C.C. Lin, L. Fan, Y. Lee, "H.ZnO-$ZnFe_2O_4$ Catalyst for

Hydrogen Production from Methanol Steam Reforming." Catalysts 13(2023)762.

[4] M. S. AlSalhi, S. Devanesan, N. Asemi, A. Ahamed, "Concurrent fabrication of ZnO–$ZnFe_2O_4$ hybrid nanocomposite for enhancing photocatalytic degradation of organic pollutants and its bacterial inactivation." Chemosphere 318 (2023) 137928.

[5] W. Zhang, X. Chen, N. Xu, R. Xiang, Y. Zhu, Z. Tang, "Morphology and optical property of zno nanostructures grown by solvothermal method: effect of the solution pretreatment." Journal of Nanomaterials (2013) 5-5.

[6] L. Xue, E. Liang, J. Wang, "Fabrication of magnetic ZnO/$ZnFe_2O_4$/diatomite composites: improved photocatalytic efficiency under visible light irradiation." Journal of Materials Science: Materials in Electronics 33 (2022) 1405-1424.

[7] P. Falak, S. A. Hassanzadeh-Tabrizi, A. Saffar-Teluri, "Synthesis, characterization, and magnetic properties of ZnO-$ZnFe_2O_4$ nanoparticles with high photocatalytic activity." Journal of Magnetism and Magnetic Materials 441(2017) 98-104.

[8] L.T. Nguyen, D.V.N. Vo, L.T. Nguyen, A.T. Duong, H.Q. Nguyen, N.M. Chu, D.T.C Nguyen, T. Van Tran, "Synthesis, characterization ,and application of $ZnFe_2O_4$@ ZnO nanoparticles for photocatalytic degradation of Rhodamine B under visible-light illumination." Environmental Technology & Innovation 25 (2022) 102130.

[9] T. Pandiyarajan, B. Karthikeyan, "Optical properties of annealing induced post growth ZnO: ZnFe2O4 nanocomposites." Spectrochimica Acta Part A: Molecular and Biomolecular Spectroscopy 106 (2013) 247-252.

[10] N.T.T. Nguyen, L.M. Nguyen, T.T.T. Nguyen, , N.H. Nguyen, D.H. Nguyen, D.T.C. Nguyen, T. Van Tran, "Green synthesis of $ZnFe_2O_4$@ ZnO nanocomposites using Chrysanthemum spp. floral waste for photocatalytic dye degradation." Journal of Environmental Management 326 (2023) 116746

[11] N. Masmali, Z. Osman, and A. K. Arof, "Comparison between silver sulfide and cadmium sulfide quantum dots in ZnO and ZnO/$ZnFe_2O_4$ photoanode of quantum dots sensitized solar cells." Ionics 28 (2020) 2007-2020.

[12] M. Chakraborty, D. Roy, A. Sharma, R. Thangavel, "Post-treatment with $ZnFe_2O_4$ nanoparticles to improve photo-electrochemical performance of ZnO nanorods based photoelectrodes." Solar Energy Materials and Solar Cells 200(2019). 109975.

[13] M. Shekofteh-Gohari, A. Habibi-Yangjeh, M. Abitorabi, A. Rouhi, "Magnetically separable nanocomposites based on ZnO and their applications in photocatalytic processes: a review." Critical reviews in environmental science and technology 48 (2018) 806-857.

[14.] O. Al Haiqi, A.H. Nour, B.V. Ayodele, R. Bargaa "Interaction Effect of Process Variables on Solar-Assisted Photocatalytic Phenol Degradation in Oilfield Produced Water Over ZnO/Fe_2O_3 Nanocomposites." Journal of Advanced Research in Fluid Mechanics and Thermal Sciences 78 (2021) 100-121.

[15] J. Tauc, R. Grigorovici, A. Vancu, physica status solidi 15 (1966) 627–637.

[16] A.A.A. Ahmed, Z.A. Talib, M.Z. Hussein, M.H. Flaifel, N.M. Al-Hada, "Infuence of Zn/Fe molar ratio on optical and magnetic properties of ZnO and $ZnFe_2O_4$ nanocrystal as calcined products of layered double hydroxides." Journal of Spectroscopy (2014).

[17] R.S. Yadav, I. Kuřitka, J. Vilcakova, P. Urbánek, M. Machovsky, M. Masař, M. Holek. "Structural, magnetic, optical, dielectric, electrical and modulus spectroscopic characteristics of $ZnFe_2O_4$ spinel ferrite nanoparticles synthesized via honey-mediated sol-gel combustion method." Journal of Physics and Chemistry of Solids 110 (2017) 87-99.